



## Recyclable Pd(0)-Pd(II) composites formed from Pd(II) dimers with NHC ligands under Suzuki–Miyaura conditions

Marta Górna<sup>a</sup>, Michał S. Szulmanowicz<sup>a</sup>, Andrzej Gniewek<sup>a</sup>, Włodzimierz Tylus<sup>b</sup>, Anna M. Trzeciak<sup>a,\*</sup>

<sup>a</sup> Faculty of Chemistry, University of Wrocław, 14 F. Joliot-Curie St., 50-383 Wrocław, Poland

<sup>b</sup> Wrocław University of Technology, Institute of Inorganic Technology, 27 Wybrzeże Wyspiańskiego, 50-370 Wrocław, Poland

### ARTICLE INFO

#### Article history:

Received 15 November 2014

Received in revised form

14 February 2015

Accepted 9 March 2015

Available online 17 March 2015

#### Keywords:

Nanoparticles

N-heterocyclic carbene

Palladium

Suzuki–Miyaura reaction

### ABSTRACT

Dimeric complexes of the type  $[\text{Pd}(\mu\text{-X})\text{X}(\text{NHC})_2]$  were employed in the Suzuki–Miyaura cross-coupling leading to 2-methylbiphenyl. The excellent activity of the studied dimers is perfectly illustrated by a TOF of up to  $10^6 \text{ h}^{-1}$ . Mechanistic investigations with the application of TEM, XPS, and mercury poisoning tests provided an insight into the nature of the catalytic process. Accordingly, the reduction of the dimeric palladium complex  $[\text{Pd}(\mu\text{-X})\text{X}(\text{NHC})_2]$  resulted in the formation of a composite containing Pd(0) nanoparticles protected by a layer of a Pd(II) species such as anions  $[\text{PdBr}_4]^{2-}$  or  $[\text{PdBr}_3(\text{NHC})]^-$ . The *in situ* formation of Pd(0)–Pd(II) composites resulted in the high stability of the catalytic system, which was active in ten subsequent cycles without any additional protection.

© 2015 Elsevier B.V. All rights reserved.

### Introduction

Palladium complexes bearing N-heterocyclic carbene ligands (NHC) exhibit an exceptionally high catalytic activity in cross-coupling reactions that are of practical importance in the synthesis of pharmaceuticals, fine chemicals, or natural products [1]. In this context, the Suzuki–Miyaura cross-coupling should be mentioned as an efficient method designed for the preparation of non-symmetric biaryls [2,3].

Actually, monomeric palladium complexes have found applications in a broad range of C–C cross-coupling reactions, while palladium dimers have received relatively less attention [4]. The application of dimeric complexes as catalyst precursors offers some additional advantages in comparison to monomeric analogs. The dimeric structure can be split under catalytic reaction conditions with the formation of coordinatively unsaturated intermediates suitable for the efficient activation of the organic substrates. Similarly, the high activity of PEPSSI-type complexes was explained by the creation of a free coordination place after the dissociation of the pyridine ligand [5].

For dimeric precursors, a bimetallic catalytic mechanism can also be considered, which makes possible a synergetic effect of both

metal centers [6,7]. Such an effect can facilitate the oxidative addition of an aryl halide or the transmetalation, important steps in the catalytic reaction.

The dimeric palladium complexes with bulky NHC ligands were successfully applied in the Suzuki–Miyaura [8], Heck, and Buchwald–Hartwig [9] reactions, as well as in the cross-coupling of Grignard reagents [10]. Palladium(II) hydroxide dimers were tested as the catalysts in aryl amination and the Suzuki–Miyaura reactions [11]. A dimeric acetate-bridged complex with a 1,2,3-triazol-5-ylidene ligand catalyzed the hydroarylation of alkynes with moderate efficiency [12]. Palladium dimers with phosphonium cations catalyzed the Heck reaction [13], whereas their analog with the  $\text{Bu}_4\text{N}^+$  cation found application in the oxidation of alcohols [14]. The dimeric palladium complexes with small NHC ligands were till now not tested as catalysts of C–C cross-coupling.

In this paper, we present studies on the dimeric Pd–NHC complexes of the type  $[\text{Pd}(\mu\text{-X})\text{X}(\text{NHC})_2]$  (where NHC = N-heterocyclic carbene) in the Suzuki–Miyaura reaction. The studies focused on the mechanistic aspects and identification of the palladium species formed under the catalytic reaction conditions. Understanding of such transformations is essential for the design of catalytic systems operating for a long time without deactivation. Our earlier investigations showed that monomeric palladium complexes with small NHC ligands, of the type  $[\text{PdX}_2(\text{NHC})_2]$ , are very active in the Suzuki–Miyaura cross-coupling [15]. It was also evidenced that soluble Pd(II) complexes and Pd(0) nanoparticles,

\* Corresponding author. Tel.: +48 71 3757253.

E-mail address: [anna.trzeciak@chem.uni.wroc.pl](mailto:anna.trzeciak@chem.uni.wroc.pl) (A.M. Trzeciak).

formed from these Pd–NHC precursors, participated in the catalytic process [15]. In this paper we studied transformations of Pd–NHC dimers containing NHC ligands with different steric properties. Moreover, we investigated stability of the catalytic systems based on Pd–NHC dimers in several subsequent Suzuki–Miyaura runs. In the previous reports [8] very high catalytic activity of Pd–NHC dimers was demonstrated in a single reaction however possibility of catalyst recycling was not discussed.

## Experimental

### Synthesis of $[Pd(\mu-X)X(NHC)]_2$ complexes

#### Synthesis of $[Pd(\mu-Br)Br(bmim-y)]_2$

$Pd(OAc)_2$  (0.49 g, 0.22 mmol) and  $[bmim]Br$  (0.106 g, 0.48 mmol) were placed in a Schlenk tube. The resulting mixture was heated to 55 °C along with magnetic stirring for 1.5 h. The color changed from red to orange and homogeneous phase was observed. After cooling down the mixture to RT,  $CHCl_3$  was added and the orange solution was purified on silica-gel column. The obtained solution was evaporated and the resulting oily residue was dissolved in  $CH_2Cl_2$ . Next, hexane (10 mL) was added and the two-phase mixture was left at RT. After 24 h the precipitated product was filtered off and dried in vacuo. Yield: 45%.

Crystals suitable for X-ray analysis were obtained by slow evaporation of the  $CH_2Cl_2$ /hexane solution.

$^1H$  NMR (500 MHz;  $CDCl_3$ ; TMS):  $\delta$  = 6.89 (m, 4H, CH), 4.52 (br, 4H,  $NCH_2$ ), 4.13 (s, 6H,  $CH_3$ ), 2.04 (m, 4H,  $CH_2$ ), 1.48 (m, 4H,  $CH_2$ ), 1.04 (t, 6H,  $^3J(H,H) = 7.32$  Hz, 6H;  $CH_3$ );

$^{13}C$  NMR (100 MHz,  $CDCl_3$ , TMS):  $\delta$  = 144.6 ( $N_2CH$ ), 123.4 (NCH), 122.07 (NCH), 51.1 ( $NCH_3$ ), 38.5 ( $NCH_2$ ), 32.3 ( $CH_2$ ), 19.8 ( $CH_2$ ), 13.7 ( $CH_3$ ) elemental analysis calcd (%) for  $C_{16}H_{28}Br_4N_4Pd_2$ : C 23.76, H 3.49, N 6.93; found: C 24.05, H 3.30, N 6.80.

#### Synthesis of $[Pd(\mu-Cl)Cl(bmim-y)]_2$

The method was the same as for  $[Pd(\mu-Br)Br(bmim-y)]_2$ . Yield: 52%

$^1H$  NMR (500 MHz;  $CDCl_3$ ; TMS):  $\delta$  = 6.8 (m, 4H, CH), 4.5 (br, 4H,  $NCH_2$ ), 4.1 (s, 6H,  $CH_3$ ), 2.0 (m, 4H,  $CH_2$ ), 1.4 (m, 4H,  $CH_2$ ), 1.0 (t, 6H,  $CH_3$ ,  $^3J(H,H) = 7.3$  Hz, 6H,  $CH_3$ )

$^{13}C$  NMR (100 MHz,  $CDCl_3$ , TMS):  $\delta$  = 144.5 ( $N_2CH$ ), 122.6 (NCH), 121.1 (NCH), 50.1 ( $NCH_3$ ), 37.4 ( $NCH_2$ ), 31.4 ( $CH_2$ ), 19.1 ( $CH_2$ ), 12.7 ( $CH_3$ ) elemental analysis calcd (%) for  $C_{16}H_{28}Cl_4N_4Pd_2$ : C 30.45, H 4.47, N 8.88, found: C 30.62, H 4.47, N 9.15.

#### Synthesis of $[Pd(\mu-Br)Br(emim-y)]_2$

The method was the same as for  $[Pd(\mu-Br)Br(bmim-y)]_2$ . Yield: 42%

Crystals suitable for X-ray analysis were obtained by slow evaporation of the  $CH_2Cl_2$ /hexane solution.

$^1H$  NMR (500 MHz;  $CDCl_3$ ; TMS):  $\delta$  = 1.64 (t, 6H,  $CH_3$ ,  $J_{HH} = 7.3$  Hz), 4.15 (s, 6H,  $NCH_3$ ), 4.64 (q, 4H,  $CH_2$ ,  $J_{HH} = 7.3$  Hz), 7.01 (d, 2H, NCH,  $J(H,H) = 1.8$  Hz), 7.00 (d, 2H, NCH,  $J(H,H) = 1.8$  Hz)

$^{13}C$  NMR (125 MHz;  $CDCl_3$ ; TMS):  $\delta$  = 143.9 (s,  $N_2C$ ), 124.25 (s, CH), 121.95 (s, CH), 46.68 (s,  $NCH_3$ ), 38.71 ( $CH_2$ ), 16.08 (s,  $CH_3$ ) elemental analysis calcd. (%) for  $C_{12}H_{20}Br_4N_4Pd_2$ : C 19.15, H 2.68, N 7.44; found: C 20.11, H 2.87, N 7.06;

#### Synthesis of $[Pd(\mu-Cl)Cl(SIMes)]_2$

$Pd(OAc)_2$  (0.110 g, 0.50 mmol) and SIMes.HCl (0.170 g, 0.50 mmol) were dissolved in THF (15 mL). The resulting mixture was heated to 55 °C along with magnetic stirring for 2 h. After cooling down the mixture to RT, it was purified on silica-gel column. The resulting orange solution was transferred to the Schlenk tube and the solvent was removed under vacuum. The oily residue

was dissolved in  $CH_2Cl_2$  (5 mL) and water (3–10 mL) was added to remove unreacted SIMes.HCl. Organic phase was separated and hexane (5 mL) was slowly added. After 24 h the product was filtered off and dried in vacuum. Yield: 50%.

Crystals suitable for X-ray analysis were obtained by slow evaporation of the  $CH_2Cl_2$ /hexane solution.

$^1H$  NMR (500 MHz;  $CDCl_3$ ; TMS):  $\delta$  = 6.92 (s, 8H, ArH), 6.77 (s, 8H,  $NCH_2-NCH_2$ ), 2.47 (s, 12H, p-Ar $CH_3$ ), 1.94 (s, 24H, oAr $CH_3$ )

$^{13}C$  NMR (125 MHz;  $CDCl_3$ ; TMS):  $\delta$  = 170.9 (s,  $N_2C$ ), 137.5 (s, NC), 136.1 (s, o-C $CH_3$ ), 135.7 (s, p-C $CH_3$ ), 128.8 (s, CH), 122.4 (s,  $CH_2$ ), 21.25 (s, o- $CH_3$ ), 18.9 (s, p- $CH_3$ ) elemental analysis calcd (%)  $C_{42}H_{52}Cl_4N_4Pd_2$ : C 52.14, H 5.42, N 5.79; found: C 51.15, H 5.09, N 5.30.

### Suzuki–Miyaura reaction procedure

Suzuki–Miyaura reactions were carried out in a 50 mL Schlenk tube in an air atmosphere. The solid substrates:  $NaHCO_3$  (1.7 mmol) or KOH (1.2 mmol) and phenylboronic acid (1.15 mmol, 0.133 g) or  $NaBPh_4$  (0.30 mmol, 0.095 g) were weighed and placed directly in the Schlenk tube. Next, 5 mL of the solvent (ethylene glycol or 2-propanol or 2-propanol/water 1/1) and 2-bromotoluene (1 mmol, 0.118 mL) were added. After heating the substrates to the required temperature (40 or 100 °C), the palladium complex ( $8 \times 10^{-3}$  to  $1 \times 10^{-6}$  mmol) was added. The Schlenk tube was closed with a rubber stopper, and the reaction mixture was stirred at 40 or 110 °C. After 1 h, the reactor was quickly cooled down to room temperature and the organic products were extracted with  $3 \times 3 + 1$  mL of n-hexane (5 min with intensive stirring). The extracts (10 mL) were GC-FID analyzed (Hewlett Packard 5890) with 0.076 mL of dodecane as an internal standard. The products were identified by GC–MS (Hewlett Packard 5971A).

### Reduction of $[Pd(\mu-Br)Br(bmim-y)]_2$

0.083 g (0.10 mmol)  $[Pd(\mu-Br)Br(bmim-y)]_2$  and 0.068 g KOH (1.2 mmol) and 5 mL 2-propanol were placed in a Schlenk tube. The resulting mixture was heated to 40 °C along with magnetic stirring for 1 h. The color changed from orange to silverblack. The mixture was centrifuged and decanted. Precipitated product was washed two times with 5 mL  $CH_2Cl_2$ , centrifuged and dried under nitrogen stream. elemental analysis found (%): C 6.78, H 0.91, N 0.35;

### Transmission electron microscopy

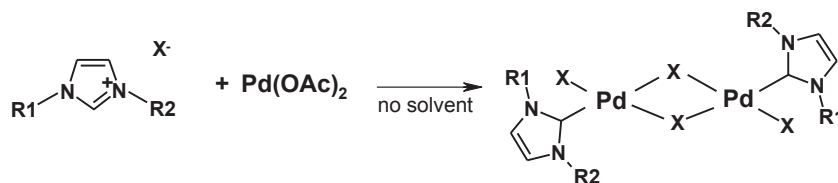
TEM measurements were carried out using a FEI Tecnai G<sup>2</sup> 20 X-TWIN electron microscope operating at 200 kV. To the sample (1–2 mg) of reduced palladium complex 2 mL of methanol were added and the resulted mixture was sonicated for 5 min. Specimens for TEM studies were prepared by putting a droplet of a colloidal suspension on a copper grid followed by evaporation the solvent under IR lamp for 15 min. The nanoparticle size distributions were determined by counting the size of approximately 250 palladium nanoparticles from several TEM images obtained from different places of the TEM grids. The size distribution plots were fitted using Gauss curve approximation.

### Crystallographic data collection and refinement

Single crystals suitable for X-ray measurements were mounted on glass fibers in silicone grease, cooled to 100 K in a nitrogen gas stream [16], and the diffraction data were collected on a Kuma KM-4 CCD diffractometer with graphite monochromated Mo-K $\alpha$  radiation ( $\lambda = 0.71073$  Å). The structures were subsequently solved using direct methods and developed by full least-squares

**Table 1**  
Crystallographic data.

Complex	$[\text{Pd}(\mu\text{-Br})\text{Br}(\text{emim-}y)]_2$	$[\text{Pd}(\mu\text{-Br})\text{Br}(\text{bmim-}y)]_2$	$[\text{Pd}(\mu\text{-Br})\text{Br}(\text{SIMes})]_2$
Formula	$[\text{Pd}_2\text{Br}_4(\text{C}_6\text{H}_{10}\text{N}_2)_2] \cdot \text{CH}_2\text{Cl}_2$	$[\text{Pd}_2\text{Br}_4(\text{C}_8\text{H}_{14}\text{N}_2)_2]$	$[\text{Pd}_2\text{Cl}_4(\text{C}_{21}\text{H}_{26}\text{N}_2)_2] \cdot \text{CHCl}_3$
$M_r$	837.69	808.86	1086.84
Crystal system	Monoclinic	Monoclinic	Monoclinic
Space group	$I2/a$	$P2_1/n$	$P2_1/c$
$a$ [Å]	14.880 (4)	7.525 (3)	14.290 (3)
$b$ [Å]	7.759 (3)	14.085 (6)	11.887 (2)
$c$ [Å]	20.983 (5)	11.344 (4)	30.984 (9)
$\beta$ [°]	105.00 (3)	108.51 (3)	116.37 (3)
$V$ [Å <sup>3</sup> ]	2340.0 (12)	1140.1 (8)	4716 (2)
$Z$	4	2	4
$D_x$ [g/cm <sup>3</sup> ]	2.378	2.356	1.531
Radiation	Mo-K $\alpha$	Mo-K $\alpha$	Mo-K $\alpha$
Reflections	12,458	9244	65,064
Parameters	146	120	517
$R_{\text{int}}$	0.025	0.047	0.107
$R_1$ ( $I > 2\sigma$ )	0.025	0.051	0.089
$wR_2$ ( $I > 2\sigma$ )	0.055	0.134	0.113
$\theta$ [°]	3.0–25.0	3.0–27.5	3.0–27.5
$\mu$ [mm <sup>-1</sup> ]	8.60	8.60	1.19
$T$ [K]	100 (2)	100 (2)	100 (2)
Color, shape	Plate, yellow	Plate, yellow	Needle, yellow
Size [mm]	0.15 × 0.15 × 0.08	0.10 × 0.10 × 0.05	0.20 × 0.10 × 0.10

**Fig. 1.** Synthesis of  $[\text{Pd}(\mu\text{-X})\text{X}(\text{NHC})]_2$  complexes.

refinement on  $F^2$ . Structural solution and refinement was carried out using SHELX suite of programs [17]. Analytical absorption corrections were performed with Crysalis RED [18]. C, N, Cl, Br and Pd atoms were refined anisotropically. All H atoms were positioned geometrically and refined isotropically using a riding model with a common fixed isotropic thermal parameter. The molecular structure plots were prepared using ORTEP-3 program [19]. Crystal data and selected details of structure determination are summarized in Table 1.

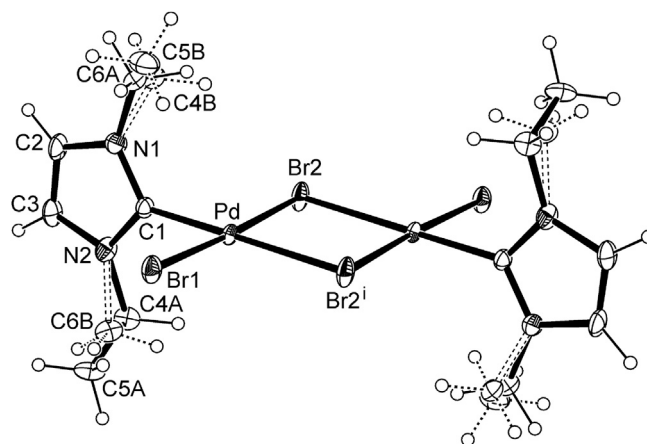
## Results and discussion

### Synthesis and structure of palladium dimers $[\text{Pd}(\mu\text{-X})\text{X}(\text{NHC})]_2$

The dimeric complexes of the type  $[\text{Pd}(\mu\text{-X})\text{X}(\text{NHC})]_2$  were obtained in reaction of  $\text{Pd}(\text{OAc})_2$  with ionic liquids (NHC-HX) under conditions similar to those reported in the literature [20] (Fig. 1). In a modified procedure, the first step of the synthesis was performed without a solvent, by mixing substrates, followed by the treatment of the resulting mixture with THF. Such a protocol enabled the increase of the yield of the product compared to that obtained in

solution. Four dimeric complexes were prepared; their composition was confirmed by elemental analyses, and a further structural characterization was based on spectroscopic and X-ray results.

In the solid state, three complexes were characterized by the X-ray single crystal analysis:  $[\text{Pd}(\mu\text{-Br})\text{Br}(\text{emim-}y)]_2$  (emim- $y$  = 1-ethyl-3-methylimidazol-2-ylidene),  $[\text{Pd}(\mu\text{-Br})\text{Br}(\text{bmim-}y)]_2$  (bmim- $y$  = 1-butyl-3-methylimidazol-2-ylidene), and  $[\text{Pd}(\mu\text{-Cl})\text{Cl}(\text{SIMes})]_2$  (SIMes = 1,3-bis(2,4,6-trimethylphenyl)-4,5-dihydroimidazol-2-ylidene). In all these complexes, the Pd–C bond length is in the

**Fig. 2.** The molecular structure and atom numbering scheme of  $[\text{Pd}(\mu\text{-Br})\text{Br}(\text{emim-}y)]_2$ . Displacement ellipsoids are drawn at the 30% probability level and H atoms are shown as small spheres of arbitrary radii. Disordered parts with lower occupancy (45%) are represented by dashed lines. Unlabeled atoms are generated by symmetry operations [symmetry code: (i)  $1 - x, -y, 1 - z$ ]. For clarity, solvent molecules have been omitted.**Table 2**  
Characteristic bond lengths (Å) observed in  $[\text{Pd}(\mu\text{-X})\text{X}(\text{NHC})]_2$  complexes.

Complex	Pd–C	Pd–( $\mu$ -X)	Pd–X
$[\text{Pd}(\mu\text{-Br})\text{Br}(\text{emim-}y)]_2$	1.952 (4)	2.5255 (8)	2.4189 (8)
$[\text{Pd}(\mu\text{-Br})\text{Br}(\text{bmim-}y)]_2$	1.924 (7)	2.4988 (8)	2.4056 (8)
$[\text{Pd}(\mu\text{-Cl})\text{Cl}(\text{SIMes})]_2$	1.947 (5)	2.332 (2)	2.294 (2)
	1.944 (5)	2.397 (2)	2.302 (2)
		2.402 (2)	
		2.328 (2)	

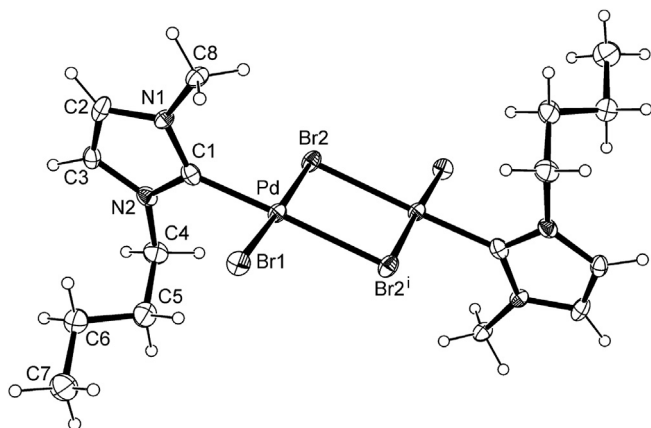


**Fig. 3.** The molecular structure and atom numbering scheme of  $[\text{Pd}(\mu\text{-Br})\text{Br}(\text{bmim-y})]_2$ . Displacement ellipsoids are drawn at the 30% probability level and H atoms are shown as small spheres of arbitrary radii. Unlabeled atoms are symmetrically dependent via inversion center [symmetry code: (i)  $1-x, 1-y, 1-z$ ].

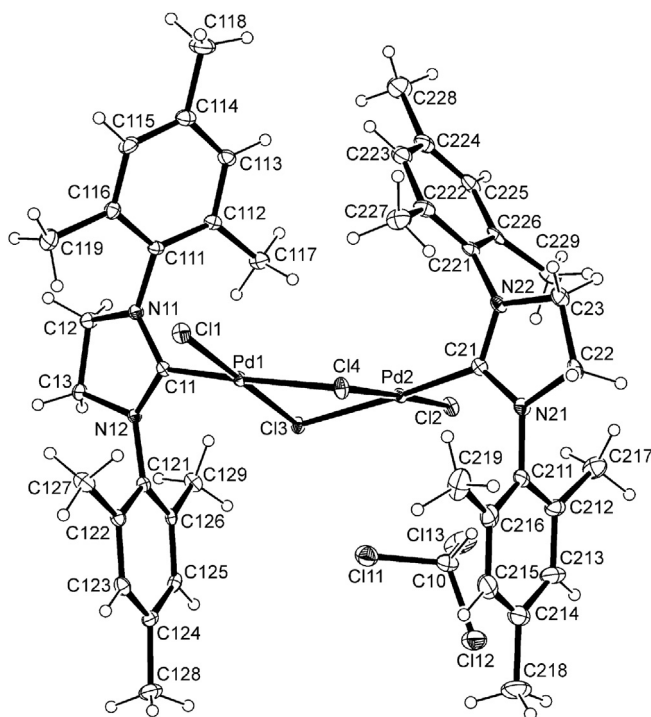


**Fig. 4.** The molecular structure and atom numbering scheme of  $[\text{Pd}(\mu\text{-Cl})\text{Cl}(\text{SiMes})_2]$ . Displacement ellipsoids are drawn at the 30% probability level and H atoms are shown as small spheres of arbitrary radii.

range of 1.92–1.95 Å (Table 2) and is not influenced by the type of substituent in the imidazolium ring. This length is characteristic for the dimeric Pd–NHC complexes [21–23]. In contrast, the Pd–C bond length in the *trans* isomers of the monomeric Pd–NHC complexes is slightly longer and is around 2.02 Å [15].

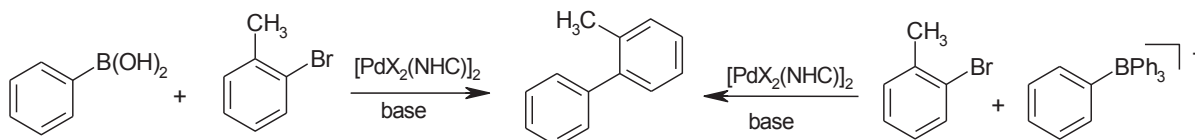


**Fig. 5.** Catalytic reactions under study.

The crystal structure of  $[\text{Pd}(\mu\text{-Br})\text{Br}(\text{emim-y})]_2$  (Fig. 2) shows a substitutional disorder of the ethyl and methyl groups with 55/45% occupancy factors. The coordination geometry of the palladium atoms is, as expected, square-planar. However, there are observed small distortions of the angles between the coordinated ligands of about  $3^\circ$  due to the influence of the bridging  $\mu\text{-Br}$  atoms. The molecular structure of  $[\text{Pd}(\mu\text{-Br})\text{Br}(\text{bmim-y})]_2$  (Fig. 3) is very similar to the structure of  $[\text{Pd}(\mu\text{-Br})\text{Br}(\text{emim-y})]_2$ .

The X-ray structure of  $[\text{Pd}(\mu\text{-Cl})\text{Cl}(\text{SiMes})_2]$  (Fig. 4) shows more significant distortions of the coordination geometry around the Pd atoms. It is especially important to notice the dihedral angle of  $28.5^\circ$  between the planes formed by  $\text{Pd1/C11/C13/C14}$  and  $\text{Pd2/C21/C12/C13/C14}$ . In  $[\text{Pd}(\mu\text{-Br})\text{Br}(\text{emim-y})]_2$  and  $[\text{Pd}(\mu\text{-Br})\text{Br}(\text{bmim-y})]_2$ , all the respective atoms were located in a planar arrangement.

#### Catalytic activity of palladium dimers in the Suzuki–Miyaura reaction

The structurally characterized Pd–NHC dimers were employed in the Suzuki–Miyaura reaction leading to 2-methylbiphenyl (Fig. 5).

Preliminary tests showed that the studied dimers offered a very good yield of the Suzuki–Miyaura product already at  $40^\circ\text{C}$  in 2-propanol or a 2-propanol/water mixture (Table 3).

Under these conditions monomeric complexes  $[\text{PdX}_2(\text{NHC})_2]$  were not active [15]. When  $\text{NaHCO}_3$  was used instead of KOH they formed 40–63% of 2-methylbiphenyl [15].

Therefore, in order to compare the efficiency of the Pd–NHC dimeric complexes with that of the  $[\text{PdX}_2(\text{NHC})_2]$  precursors [15], ethylene glycol was used as a solvent in further experiments. The results of the optimization of the reaction conditions with respect to the palladium amount are presented in Table 4.

The studied complexes produced 80–100% of 2-methylbiphenyl when used in as small amounts as  $10^{-7}$  mol. Even higher yield, close to 100%, was noted in reactions with  $\text{NaBPh}_4$  as a substrate. The excellent activity of the studied dimers is perfectly illustrated by TON values of up to  $10^6$ . As the reaction time was fixed as 1 h, the TOF values are of the same order as when expressed in  $\text{h}^{-1}$ . Interestingly, very good results were obtained for the precursor containing the bulky SiMes ligand as well as for analogs bearing the less hindered emim-y or bmim-y ligands. In fact, the catalytic results obtained with application of Pd–NHC dimers were comparable or slightly better than those achieved for Pd–NHC monomeric precursors [15]. This is in particular seen in reactions performed with the lowest concentration of palladium (0.0001 mol%). The yield obtained with monomeric Pd–NHC complexes was 2–76%, and 86% was obtained with  $[\text{Pd}(\text{IMes})_2\text{Cl}_2]$ . The studied dimers provided 81–90% under the same conditions. Importantly, the presented systems perfectly operated in air atmosphere without any catalyst pretreatment.

#### Recycling experiments

To prove the stability of our system, we performed several consecutive reactions using one portion of  $[\text{Pd}(\mu\text{-Br})\text{Br}(\text{bmim-y})]_2$ . After each reaction, the mixture was centrifuged and the black

**Table 3**  
Yield of 2-methylbiphenyl obtained in the Suzuki–Miyaura cross-coupling with  $[\text{Pd}(\mu\text{-X})(\text{NHC})_2]$  catalysts.

Catalyst	Yield [%]	
	2-Propanol	2-Propanol/water
$[\text{Pd}(\mu\text{-Br})\text{Br}(\text{bmim-}y)_2]$	82	84
$[\text{Pd}(\mu\text{-Cl})\text{Cl}(\text{bmim-}y)_2]$	69	88

Reaction conditions:  $[\text{Pd}]$  1% mol; 2-Br-toluene 1 mmol,  $\text{PhB}(\text{OH})_2$  1.1 mmol,  $\text{KOH}$  1.2 mmol, 1 h, 40 °C.

**Table 4**  
Yield of 2-methylbiphenyl obtained in the Suzuki–Miyaura cross-coupling with different amounts of  $[\text{Pd}(\mu\text{-X})(\text{NHC})_2]$  catalysts.

Catalyst	$[\text{Pd}]$ [mol%]	$\text{PhB}(\text{OH})_2$	$\text{NaBPh}_4$
		Yield [%]	Yield [%]
$[\text{Pd}(\mu\text{-Br})\text{Br}(\text{bmim-}y)_2]$	0.8	83	99
	0.01	90	99
	0.0001	86	98
$[\text{Pd}(\mu\text{-Br})\text{Br}(\text{emim-}y)_2]$	0.8	87	99
	0.01	97	99
	0.0001	90	99
$[\text{Pd}(\mu\text{-Cl})\text{Cl}(\text{SImes})_2]$	0.8	100	98
	0.01	90	90
	0.0001	81	98

Reaction conditions:  $[\text{Pd}]$  0.8–0.0001% mol; 2-Br-toluene 1 mmol,  $\text{PhB}(\text{OH})_2$ ,  $\text{NaBPh}_4$  1.15 mmol,  $\text{NaHCO}_3$  1.7 mmol, 1 h, 110 °C.

precipitate containing palladium was washed with 2-propanol, dried, and used in the next run. It is worth noting that experiments were performed in air and the recovered catalyst was also stored in contact with air between reactions. Although a significant amount of palladium was lost during the experiments, in particular soluble palladium species were washed out, ten runs were successfully performed (Fig. 6). The yield of 2-methylbiphenyl changed from 91% in the first reaction to 55% in the last one, indicating a very high stability of the system. In fact, there is the first example of the efficient recycling of the not-stabilized Pd–NHC catalyst.

#### Formation of Pd(0) nanoparticles

During catalytic experiments, the formation of black palladium was observed, indicating palladium reduction. Several attempts were undertaken to explain the course of this process and the role

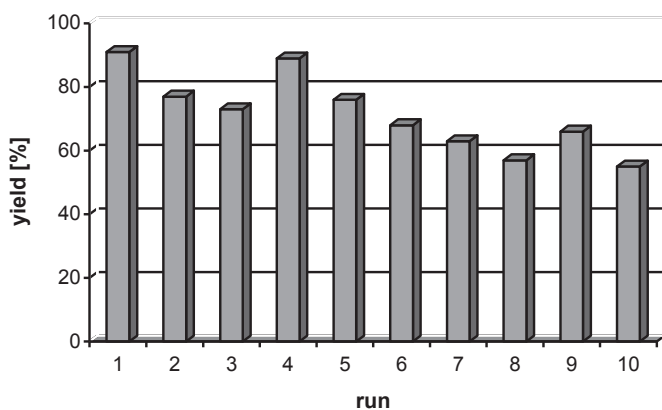


**Fig. 6.** Consecutive Suzuki–Miyaura reactions performed with  $[\text{Pd}(\mu\text{-Br})\text{Br}(\text{bmim-}y)_2]$  recovered after each run. Reaction conditions:  $[\text{Pd}]$  1% mol; 2-Br-toluene 1 mmol,  $\text{PhB}(\text{OH})_2$  1.1 mmol,  $\text{KOH}$  1.1 mmol, 1 h, 70 °C, 2-propanol/water 1/1.

**Table 5**  
Size of Pd(0) nanoparticles formed in ethylene glycol and in the Suzuki–Miyaura reaction.

Complex	Average diameter of Pd(0) nanoparticles [nm]	
	Ethylene glycol	Suzuki–Miyaura reaction
$[\text{Pd}(\mu\text{-Br})\text{Br}(\text{bmim-}y)_2]$	5.7	2.9
$[\text{Pd}(\mu\text{-Br})\text{Br}(\text{emim-}y)_2]$	5.5	3.0
$[\text{Pd}(\mu\text{-Cl})\text{Cl}(\text{SImes})_2]$	4.4	4.4

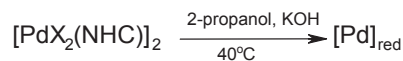


**Fig. 7.** Reduction of Pd–NHC dimer.

of Pd(0) in the reaction course. It was found that heating of the dimeric complexes  $[\text{Pd}(\mu\text{-X})(\text{NHC})_2]$  in ethylene glycol resulted in the formation of Pd(0) nanoparticles with the average diameter of 4.4–5.7 nm, as estimated by TEM. Interestingly, when the dimeric complexes were heated in ethylene glycol in the presence of all of the Suzuki–Miyaura reactants, slightly smaller nanoparticles were formed (Table 5). Thus, considering the decrease in size, it can be supposed that the nanoparticles were solubilized in contact with the components of the reaction mixture and formed molecular palladium species. Possibility of transformation of Pd(0) nanoparticles into Pd(II) complexes under catalytic reaction conditions was also discussed by other authors [20]. It can also be deduced from the size of nanoparticles that their aggregation is diminished in the presence of Suzuki–Miyaura substrates. Accordingly, Pd(0) nanoparticles produced *in situ* can be considered a reservoir of soluble catalytically active palladium forms [15]. In agreement with such a supposition in a case of studied dimers was the result of the Hg(0) test, in which the inhibiting effect was not observed at a 100-fold excess of Hg(0) in relation to palladium. It is accepted in the literature that Hg(0) interacts with Pd(0) or an underligated palladium species forming an amalgam which does not contribute to the catalytic process. When the inhibition is not observed, it might be proposed that Pd(0) nanoparticles do not represent the catalytically active form [21].

#### Reduction of Pd(II) precursors

In order to learn more about the nature of Pd(0) nanoparticles in the studied systems, additional experiments with the reduction of the dimeric complex  $[\text{Pd}(\mu\text{-Br})\text{Br}(\text{bmim-}y)_2]$  were undertaken. It was found that warming the dimer  $[\text{Pd}(\mu\text{-Br})\text{Br}(\text{bmim-}y)_2]$  in 2-propanol at 40 °C did not cause palladium reduction. However, the same procedure carried out in the presence of  $\text{KOH}$  resulted in the formation of a black solution with some amount of a precipitate (Fig. 7).

**Table 6**  
The yield of the Suzuki–Miyaura cross-coupling in ethylene glycol catalyzed by  $[\text{Pd}]_{\text{red}}$  obtained according to Fig. 7.

Amount of Pd [mol%]	Yield [%]
0.25	91
0.5	90
0.75	91
1	93
2	66

Reaction conditions: 2-Br-toluene 1 mmol;  $\text{PhB}(\text{OH})_2$  1.15 mmol,  $\text{KOH}$  1 mmol, ethylene glycol 5 mL, 110 °C, 1 h.

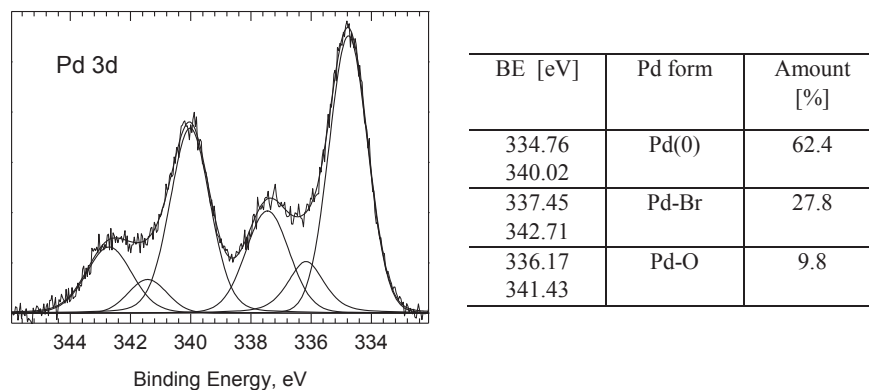


Fig. 8. XPS data for the  $[\text{Pd}]_{\text{red}}$  obtained by reduction of  $[\text{Pd}(\mu\text{-Br})\text{Br}(\text{bmim-}y)]_2$  in 2-propanol/KOH.

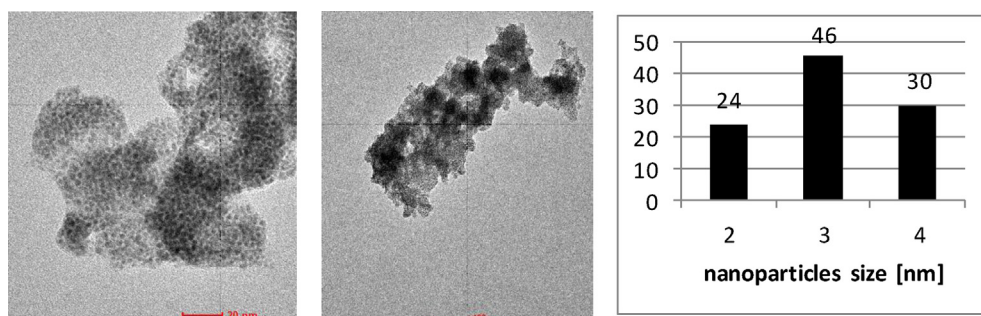


Fig. 9. TEM data for the  $[\text{Pd}]_{\text{red}}$  obtained by reduction of  $[\text{Pd}(\mu\text{-Br})\text{Br}(\text{bmim-}y)]_2$  in 2-propanol/KOH.

A sample of the reduced palladium ( $[\text{Pd}]_{\text{red}}$ ) was obtained by heating the  $[\text{Pd}(\mu\text{-Br})\text{Br}(\text{bmim-}y)]_2$  complex with a 10-fold excess of KOH at 40 °C in 2-propanol for 1 h. Interestingly, the resulting black powder efficiently catalyzed the Suzuki–Miyaura coupling, leading to 93% product yield in 1 h Table 6 presents the results of the catalytic reactions performed with the application of different amounts of reduced palladium,  $[\text{Pd}]_{\text{red}}$ . High yields of the product were noted for 0.25–1% mol of palladium, while for 2% mol, the yield of 2-methylbiphenyl decreased to 66%. It may be assumed that the faster agglomeration of palladium probably inhibited the catalytic reaction at a higher concentration [22].

The product of the reduction of  $[\text{Pd}(\mu\text{-Br})\text{Br}(\text{bmim-}y)]_2$  in 2-propanol,  $[\text{Pd}]_{\text{red}}$ , was analyzed using the XPS and TEM methods in order to estimate its composition. The complete reduction of

$\text{Pd(II)}$  to  $\text{Pd(0)}$  was expected; however, it was not the case, and, according to XPS data, not only  $\text{Pd(0)}$  but also  $\text{Pd(II)}$  species were found in the analyzed sample. Representative XPS data of the sample of  $[\text{Pd}]_{\text{red}}$  are presented in Fig. 8. Two forms of  $\text{Pd(II)}$  were observed, namely ones containing  $\text{Pd-Br}$  and  $\text{Pd-O}$  bonds. The presence of  $\text{Pd-Br}$  bondings is consistent with XPS Br 3d spectrum showing binding energy (BE) of Br 3d<sub>5/2</sub> 68 eV, very close to that estimated for  $[\text{Bu}_4\text{N}]_2[\text{PdBr}_4]$ , 67.95 eV [23]. The presence of  $\text{Pd(0)}$  nanoparticles was also confirmed by TEM measurements in the same sample (Fig. 9).

On the basis of the obtained results, it can be assumed that the reduction of the  $\text{Pd-NHC}$  complexes resulted in the formation of a composite containing  $\text{Pd(0)}$  nanoparticles protected by a layer of a cationic and an anionic palladium species,  $[\text{PdBr}(\text{NHC})]^+$  and

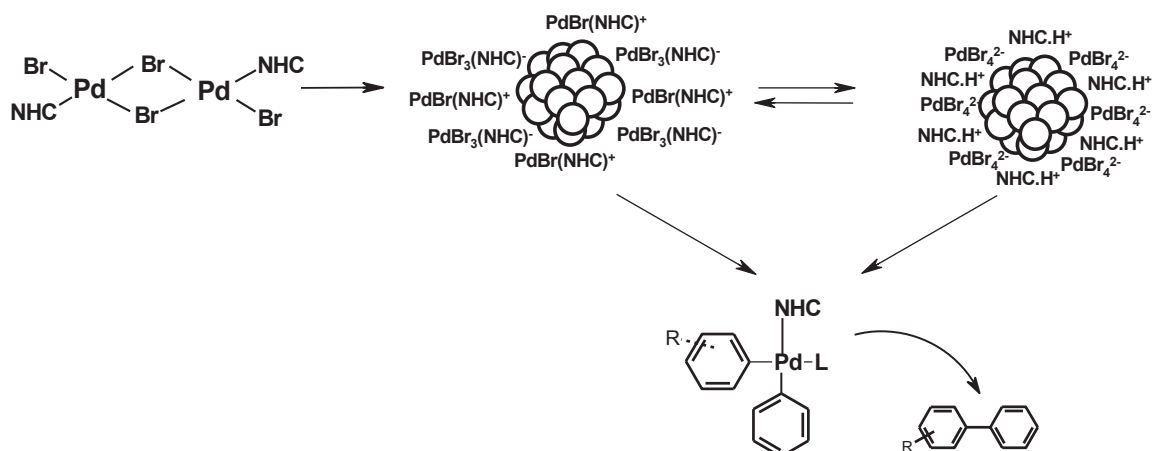


Fig. 10. Plausible transformations of  $[\text{Pd}(\mu\text{-Br})\text{Br}(\text{bmim-}y)]_2$  during Suzuki–Miyaura conditions.

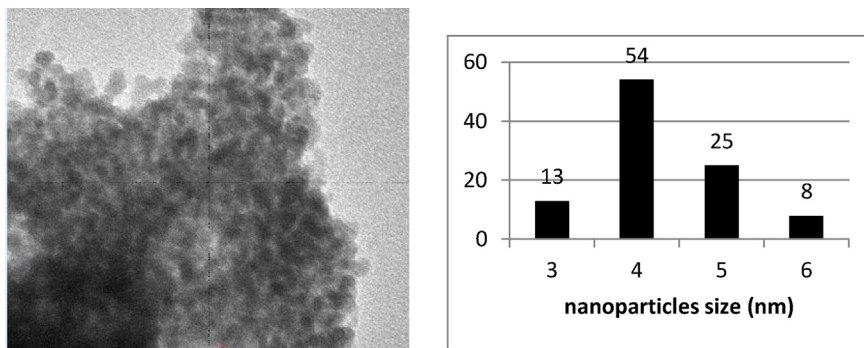


Fig. 11. TEM data for the palladium residue recovered after 10 runs of Suzuki–Miyaura reactions catalyzed by  $[\text{Pd}(\mu\text{-Br})\text{Br}(\text{bmim-}y)]_2$ .

$[\text{PdBr}_3(\text{NHC})]^-$ . The protective shell can also contain imidazolium cations  $[\text{NHC}\cdot\text{H}]^+$  and  $[\text{PdBr}_4]^{2-}$  anions (Fig. 10). The presence of NHC and  $\text{X}^-$  ligands released when Pd(0) nanoparticles were formed facilitated formation of anionic and cationic Pd(II) species.

A core–shell structure presented on Fig. 10 is similar to that proposed for the product obtained by the reduction of  $\text{Pd}(\text{OAc})_2$  by tetrabutylammonium acetate [24]. Under catalytic reaction conditions the additional stabilization of Pd(0) nanoparticles by NHC ligands should also be considered. For example, the formation of the self-assembled NHC monolayer on the surface of Au(0) nanoparticles was recently evidenced [25].

The palladium-containing residue isolated after ten recycling experiments was analyzed for comparison using the TEM method. TEM micrographs show small Pd(0) nanoparticles with a diameter of ca. 4 nm, distributed uniformly without significant agglomeration (Fig. 11). The size of the nanoparticles is very close to that estimated after one Suzuki–Miyaura reaction as well as after the reduction of the precursor in 2-propanol/KOH. Considering the fact that the recycling experiments (presented in Fig. 6) were performed without any additional stabilizing agents, the high stability of the nanoparticles against agglomeration is worth underlining. In our opinion, the formation of Pd(0)–Pd(II) composites can rationalize the observed feature.

## Conclusions

Palladium(II) dimers,  $[\text{Pd}(\mu\text{-X})\text{X}(\text{NHC})]_2$ , showed an excellent catalytic activity in Suzuki–Miyaura reactions, characterized by a TOF of up to  $10^6 \text{ h}^{-1}$ . Transformations of the catalyst precursor to a Pd(0)–Pd(II) composite creates a very stable system, which is highly efficient in several subsequent runs of the Suzuki–Miyaura reaction. During a catalytic reaction, the Pd(II) species present on the surface of the composite can be easily transferred into the solution and take part in the catalytic transformations. This is illustrated in Fig. 10 by the schematic activation of the substrate on a single palladium ion leached from the composite. Pd(0) nanoparticles forming the core of the composite undergo solubilization during the reaction, which is in fact catalyzed by molecular palladium species. At the end of the catalytic cycle, palladium is reduced and new nanoparticles are formed.

Therefore, the continuous transformations of Pd(II) to Pd(0) and the oxidation of Pd(0) to Pd(II) have fundamental influence on the reaction course, preventing the formation of inactive palladium black. The catalytic system operating according to the described model is active for more than one catalytic cycle and for a relatively long time.

Interestingly, the stabilizing shell composed of Pd(II) species protects the Pd(0) nanoparticles against agglomeration very well. In our opinion, the presence of the NHC ligands as well as their

protonated forms (NHC·HX) are of fundamental importance for the observed long-term activity of the palladium systems.

## Acknowledgments

Financial support of National Science Foundation (NCN) with grant 2012/05/B/ST5/00265 is gratefully acknowledged (MG, AG, AMT).

## Appendix A. Supplementary material

CCDC reference codes: 997186–997188 contain the supplementary crystallographic data for this paper. These data can be obtained free of charge from The Cambridge Crystallographic Data Centre via [www.ccdc.cam.ac.uk/data\\_request/cif](http://www.ccdc.cam.ac.uk/data_request/cif).

## References

- [1] a) N-heterocyclic carbenes in transition metal catalysis, in: F. Glorius (Ed.), *N-Heterocyclic Carbenes in Synthesis*, Springer-Verlag, Berlin, Germany, 2007; S.P. Nolan Ed., Wiley-VCH, New York, 2006; b) C.M. Crudden, D.P. Allen, *Coord. Chem. Rev.* 248 (2004) 2247–2273; c) W.A. Herrmann, C. Köcher, *Angew. Chem. Int. Ed.* 36 (1997) 2162–2187; d) E.A.B. Kantchev, C.J. O'Brien, M.G. Organ, *Aldrichim. Acta* 39 (2006) 97–111; e) S. Chowdhury, R.S. Mohan, L. Scott, *Tetrahedron* 63 (2007) 2363–2389; f) N. Marion, S.P. Nolan, *Acc. Chem. Res.* 41 (11) (2008) 1440–1449; g) N.M. Scott, S.P. Nolan, *Eur. J. Inorg. Chem.* (2005) 1815–1828; h) F. Bellina, A. Carpita, R. Rossi, *Synthesis* 15 (2004) 2419–2440; i) F.E. Hahn, M.C. Jahnke, *Angew. Chem. Int. Ed.* 47 (2008) 3122–3172; j) W.J. Sommer, M. Weck, *Coord. Chem. Rev.* 251 (2007) 860–873; k) K. Arentsen, S. Caddick, F.G.N. Cloke, *Tetrahedron* 61 (2005) 9710–9715.
- [2] a) N. Miyaura, A. Suzuki, *Chem. Rev.* 95 (1995) 2457–2483; b) A. Suzuki, *J. Organomet. Chem.* 576 (1999) 147–168; c) N. Miyaura, *Top. Curr. Chem.* 219 (2002) 11–59.
- [3] a) C. Torborg, M. Beller, *Adv. Synth. Catal.* 351 (2009) 3027–3043; b) J. Magano, J.R. Dunetz, *Chem. Rev.* 111 (2011) 2177–2250.
- [4] V.P. Ananikov, S.S. Zaleskiy, V.V. Kachala, I.P. Beletskaya, *J. Organomet. Chem.* 696 (2011) 400–405.
- [5] C. Valente, S. Calimsiz, K.H. Hoi, D. Mallik, M. Sayah, M.G. Organ, *Angew. Chem. Int. Ed.* 51 (2012) 3314–3332.
- [6] V.P. Ananikov, I.P. Beletskaya, *Organometallics* 31 (2012) 1595–1604.
- [7] A.S. Kashin, V.P. Ananikov, *J. Org. Chem.* 78 (22) (2013) 11117–11125.
- [8] O. Diebolt, P. Braunstein, S.P. Nolan, C.S.J. Cazin, *ChemComm* (2008) 3190–3192.
- [9] U.I. Tessin, X. Bantreil, O. Songis, C.S.J. Cazin, *Eur. J. Inorg. Chem.* (2013) 2007–2010.
- [10] C.E. Hartmann, S.P. Nolan, C.S.J. Cazin, *Organometallics* 28 (2009) 2915–2919.
- [11] J.D. Egbert, A. Chartoire, A.M.Z. Slawin, S.P. Nolan, *Organometallics* 30 (2011) 4494–4496.
- [12] R. Saravankumar, V. Ramkumar, S. Sankararaman, *Organometallics* 30 (2011) 1689–1694.
- [13] A.R. Hajipour, G. Azizi, *SynLett.* 24 (2) (2013) 254–258.
- [14] J. Bouquillon, A.M. d'Hardemare, M.-T. Averbuch-Puchot, F. Henin, J. Muzart, *Polyhedron* (1999) 3511–3516.
- [15] M.S. Szulmanowicz, A. Gniewek, W. Gil, A.M. Trzeciak, *ChemCatChem* 5 (2013) 1152–1160.
- [16] J. Cosier, A.M. Glazer, *J. Appl. Cryst.* 19 (1986) 105–107.
- [17] G.M. Sheldrick, *Acta Crystallogr. Sect. A* 64 (2008) 112–122.

- [18] Oxford Diffraction, CrysAlis RED Version 1.171.33.55, Oxford Diffraction Ltd, Wrocław, Poland, 2008.
- [19] L.J. Farrugia, *J. Appl. Crystallogr.* 30 (1997) 565.
- [20] a) M. Perez-Lorenzo, *J. Phys. Chem. Lett.* 3 (2012) 167–174;  
b) C.-J. Jia, F. Schüth, *Phys. Chem. Chem. Phys.* 13 (2011) 2457–2487;  
c) A. Balanta, C. Godard, C. Claver, *Chem. Soc. Rev.* 40 (2011) 4973–4985.
- [21] a) N.T.S. Phan, M. van der Sluys, C.W. Jones, *Adv. Synth. Catal.* 348 (2006) 609–679;  
b) R.H. Crabtree, *Chem. Rev.* 112 (2012) 1536–1554.
- [22] J.G. de Vries, *Dalton Trans.* (2006) 421–429.
- [23] A. Gniewek, A.M. Trzeciak, J.J. Ziótkowski, L. Kępiński, J. Wrzyszc, W. Tylus, *J. Catal.* 229 (2005) 332.
- [24] a) V. Calo, A. Nacci, A. Monopoli, F. Montingelli, *J. Org. Chem.* 70 (2005) 6040–6044;  
b) V. Calo, A. Nacci, A. Monopoli, A. Fornaro, L. Sabbatini, N. Cioffi, N. Ditaranto, *Organometallics* 23 (2004) 5154–5158;  
c) T.M. Reetz, M. Maase, *Adv. Mater.* 11 (1998) 773–777.
- [25] C.M. Crudden, J.H. Horton, I.I. Ebralidze, O.V. Zenkina, A.B. McLean, B. Drevniok, Z. She, H.-B. Kraatz, N.J. Mosey, T. Seki, E.C. Keske, J.D. Leake, A. Rousina-Webb, G. Wu, *Nat. Chem.* 6 (2014) 409–414.